

# Flux-free conductance modulation in a helical Aharonov-Bohm interferometer

Hisao Taira<sup>1,2,3)</sup> and Hiroyuki Shima<sup>1,2)</sup>

<sup>1)</sup> Department of Applied Physics, Graduate School of Engineering, Hokkaido University, Sapporo 060-8628, Japan

<sup>2)</sup> Department of Applied Mathematics 3, LaCàN, Universitat Politècnica de Catalunya (UPC), Barcelona 08034, Spain

<sup>3)</sup> Department of Physics, The Chinese University of Hong Kong (CUHK), Shatin, New Territories, Hong Kong

E-mail: [taira@eng.hokudai.ac.jp](mailto:taira@eng.hokudai.ac.jp)

**Abstract.** A novel conductance oscillation in a twisted quantum ring composed of a helical atomic configuration is theoretically predicted. Internal torsion of the ring is found to cause a quantum phase shift in the wavefunction that describes the electron's motion along the ring. The resulting conductance oscillation is free from magnetic flux penetrating inside the ring, which is in complete contrast with the ordinary Aharonov-Bohm effect observed in untwisted quantum rings.

## 1. Introduction

The Aharonov-Bohm (AB) effect is a pivotal manifestation of geometric phase governing quantum dynamics [1]. It occurs when a charged particle travels along a coherent loop threaded by external magnetic flux; the particle's wave function acquires an additional quantum phase that influences an interference pattern. Experimental efforts to confirm its topological nature [2, 3] as well as possible applications toward quantum computations [4, 5] have made it a topic of more broader interest than ever [6, 7].

The AB effect was originally predicted for charged particles moving around magnetic flux. Since then, it has been generalized to neutral particles having magnetic [8, 9, 10] or electric [11, 12] dipole momenta that travel around a line of electric or magnetic charges, respectively. A unified picture for the three phenomena was established in the framework of the electromagnetic duality, which further predicted another interference phenomenon called the dual AB effect [13]. It is noteworthy that the AB effect has many analogues; in fact, light penetrating through an optical medium [14], quasiparticles moving in Bose-Einstein condensates [15, 16, 17, 18], and particles in a gravitational background [19, 20, 21] have been suggested to exhibit AB-like phenomena. In addition, recent attempts to reveal the Dirac fermion dynamics in the AB ring [22] and to unveil the ponderomotive AB effect driven by laser pulses [23] are quite intriguing. The series of work evidences the relevance of the effect to diverse fields in physics.

In the present paper, we propose a distinct class of the AB-like interference effect for non-interacting charged particles that moves along a helical circuit, i.e., a quantum ring consisting of helical atomic structure. Surprisingly, the effect requires no magnetic flux threading inside the ring, which is in complete contrast to the ordinary AB effect. Such the flux-free interference effect originates from a torsion-induced vector potential  $\mathbf{A}_{\text{eff}}$  that appears in the effective Hamiltonian describing the particle's motion along the helical circuit [24, 25, 26]; a similar torsion-induced effect was found in twisted optical waveguides [27]. We demonstrate that an additional phase associated with  $\mathbf{A}_{\text{eff}}$  results in a conductance oscillation whose pattern is determined by the helicity of the atomic configuration.

## 2. Basic equation and electronic eigenstates

We consider a twisted quantum ring that has the ring radius  $R_1$  and a uniform circular cross section with the tube radius  $R_2$  ( $\ll R_1$ ). The ring is composed of a helical atomic configuration around the centroidal axis  $C$  parametrized by  $q_0$ . Using an appropriate reference frame  $(q_0, q_1, q_2)$ , a point in the vicinity of  $C$  is represented by  $\mathbf{R} = \mathbf{r}(q_0) + q_1 \mathbf{e}_1(q_0) + q_2 \mathbf{e}_2(q_0)$ , where the set  $(\mathbf{e}_0, \mathbf{e}_1, \mathbf{e}_2)$  with  $\mathbf{e}_0 \equiv \partial_0 \mathbf{R}$  and  $|\mathbf{e}_1| = |\mathbf{e}_2| = 1$  forms a right-handed orthogonal triad and  $\partial_a \equiv \partial/\partial q_a$  ( $a = 0, 1, 2$ ). The vectors  $\mathbf{e}_1$  and  $\mathbf{e}_2$  rotate along  $C$  with the same rotation rate as that of helical atomic configuration, as a result of which the torsion,  $\tau \equiv \mathbf{e}_2 \cdot \partial_0 \mathbf{e}_1$ , of the reference frame equals the internal torsion of the atomic configuration. Such the twisted reference

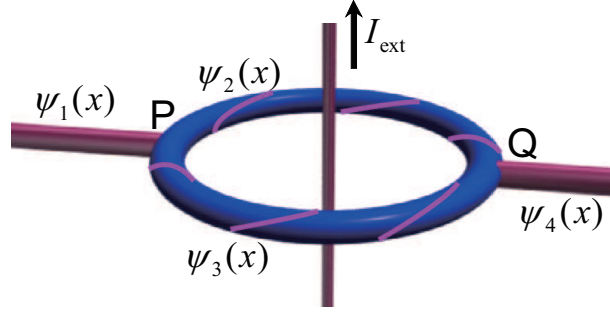


**Figure 1.** Two terminal electron interferometer based on a twisted quantum ring encircling external current flow  $I_{\text{ext}}$ . Each wavefunction  $\psi_s(x)$  ( $s = 1, 2, 3, 4$ ) describes the electron's motion lying at the lead ( $s = 1, 4$ ) or the arc ( $s = 2, 3$ ) as indicated in the figure.

frame can be useful for analyzing physical properties of actual twisted nanowires that were experimentally fabricated [28, 29] or theoretically suggested [30, 31, 32, 33, 34].

Using the twisted reference frame, the motion of non-interacting electrons is written by the Schrödinger equation such as [35, 36]

$$\mu \sum_{a,b=0}^2 \frac{1}{\sqrt{g}} \partial_a (\sqrt{g} g^{ab} \partial_b) \phi + V \phi = E \phi, \quad (1)$$

where  $\mu \equiv -\hbar^2/(2m^*)$  with an effective mass  $m^*$  and

$$g = \det[g_{ab}], \quad g_{ab} = \partial_a \mathbf{R} \cdot \partial_b \mathbf{R}, \quad g^{ab} = g_{ab}^{-1}. \quad [a, b = 0, 1, 2] \quad (2)$$

In equation (1),  $V$  represents a potential that confines the transverse motion of electrons within the cross section. Components of the tensor  $g_{ab}$  in equation (2) are given by

$$\begin{aligned} g_{00} &= \gamma^4 + \tau^2 (q_1^2 + q_2^2), & g_{01} &= g_{10} = -\tau q_2, & g_{02} &= g_{20} = \tau q_1, \\ g_{ij} &= \delta_{ij}, & [i, j &= 1, 2], \end{aligned} \quad (3)$$

where  $\gamma = \sum_{i=1}^2 (1 - \kappa_i q_i)^{1/2}$  and  $\kappa_i = \mathbf{e}_0 \cdot \partial_0 \mathbf{e}_i$ . The elements  $g^{ab}$  are those of the  $3 \times 3$  matrix  $[g^{ab}]$  inverse to  $[g_{ab}]$ , and thus they can read as

$$\begin{aligned} g^{00} &= \gamma^{-4}, & g^{01} &= g^{10} = \gamma^{-4} \tau q_2, & g^{02} &= g^{20} = -\gamma^{-4} \tau q_1, \\ g^{ij} &= \delta_{ij} + \gamma^{-4} \tau^2 \left[ (q_1^2 + q_2^2) \delta_{ij} - q_i q_j \right]. \end{aligned} \quad (4)$$

For simplicity, we assume that geometric deviation of the twisted frame from the orthogonal one is sufficiently smooth and small so that  $(\kappa_1^2 + \kappa_2^2)^{1/2} R_2 \ll 1$  and  $\tau R_2 \ll 1$ . These assumptions allow to obtain [24, 37]

$$\mu \left[ \partial_1^2 + \partial_2^2 + \left( \partial_0 - \frac{i\tau L}{\hbar} \right)^2 + \frac{1}{4R_1^2} \right] \phi + V \phi = E \phi, \quad (5)$$

where  $L \equiv -i\hbar(q_1 \partial_2 - q_2 \partial_1)$  is the angular momentum operator in the cross section. Eigenfunctions of the equation (5) have the form

$$\phi(q_0, q_1, q_2) = \psi(q_0) \sum_{n=1}^N c_n u_n(q_1, q_2). \quad (6)$$

Here,  $u_j(q_1, q_2)$  are  $N$ -fold eigenfunctions in the cross section ‡ and  $\psi(q_0)$  describes the axial motion of electrons along the twisted wire. It follows from equations (5) and (6) that  $\psi(q_0)$  obeys the effective one-dimensional Schrödinger equation such as

$$\mu \left[ \left( \partial_0 - \frac{i\tau \langle L \rangle}{\hbar} \right)^2 + \frac{1}{4R_1^2} - \frac{\tau^2}{\hbar^2} (\langle L^2 \rangle - \langle L \rangle^2) \right] \psi(q_0) = \epsilon \psi(q_0), \quad (7)$$

The angular brackets  $\langle \dots \rangle$  in equation (7) indicate to take an expectation value with respect to the two-dimensional ground-state function in the cross section. We see from equation (7) that the product  $\tau \langle L \rangle / \hbar$  plays a role of the effective vector potential  $\mathbf{A}_{\text{eff}}$  we have mentioned earlier. Hence, nonzero values of  $\tau$  and  $\langle L \rangle$  are expected to yield a quantum phase shift in the wavefunction  $\psi(q_0)$ , which originates from the helical atomic configuration in the ring. If the ring has non-uniform cross section, equation (7) contains a spatially dependent scalar potential that stems from the geometric curvature of the cylindrical surface of the ring [38, 39, 40, 41]. This potential, nevertheless, requires no qualitative revision in the conclusion of this paper.

To obtain a finite  $\langle L \rangle$ , we suppose an external current  $I_{\text{ext}}$  that penetrates through the center of the ring as shown in figure 1. The operator  $L$  is then given by  $L = -i\hbar \partial / \partial \theta - eB(q_1^2 + q_2^2) / 2$ , where  $\theta$  is the angular coordinate in the cross section,  $B = \mu_0 I_{\text{ext}} / \ell$ ,  $\ell = 2\pi R_1$  and  $\mu_0$  is the permeability of vacuum. We also assume a constant  $\tau$  throughout the ring and a parabolic potential well  $V(q_1, q_2) = m^* \omega_p^2 (q_1^2 + q_2^2) / 2$  that strongly confines the transverse motions of electrons within the cross section of radius  $R_2 \ll R_1$ ; the parameter  $\omega_p$  determines the steepness of the potential. These assumptions allow to write eigenfunctions of equation (7) as [37]

$$\psi(q_0) = \psi_{\text{unt}}(q_0) \exp \left( -\frac{i\tau}{\hbar} \int_0^{q_0} \langle L \rangle dq'_0 \right), \quad (8)$$

where  $\psi_{\text{unt}}$  is an eigenfunction for an untwisted quantum ring (i.e.,  $\tau = 0$ ). The ground-state function  $u_g(q_1, q_2)$  in the cross section reads [42, 43]

$$u_g(q_1, q_2) = \frac{1}{\sqrt{\pi} \ell_\Omega} \exp \left( -\frac{q_1^2 + q_2^2}{2\ell_\Omega} \right), \quad (9)$$

where  $\ell_\Omega = \sqrt{\hbar / (m^* \Omega)}$ ,  $\Omega = \sqrt{\omega_p^2 + (\omega_c / 2)^2}$  and  $\omega_c = eB / m^*$  is the cyclotron frequency. Then, we can prove that

$$\frac{\langle L \rangle}{\hbar} = -\frac{I_{\text{ext}}}{I_0} \frac{1}{\sqrt{4 + \left( \frac{I_{\text{ext}}}{I_0} \right)^2}}, \quad I_0 = \frac{m^* \omega_p \ell}{e \mu_0}. \quad (10)$$

Equations (8) and (10) state that nonzero  $I_{\text{ext}}$  gives rise to quantum phase shift by  $\tau \langle L \rangle \ell / \hbar$  in the eigenstate  $\psi(q_0)$ , in which the magnitude of the shift is determined by the formula (10).

Figure 2 shows how  $\langle L \rangle$  depends on the external current  $I_{\text{ext}}$  normalized by  $I_0$ .  $\langle L \rangle$  decreases monotonically with increasing  $I_{\text{ext}}$ , while it converges to  $-\hbar$  (or  $+\hbar$ ) in the

‡ The value of  $N$  depends on the eigenenergy  $E$  of equation (5) to which  $\phi$  belongs, and also on the shape of the cross section in general.

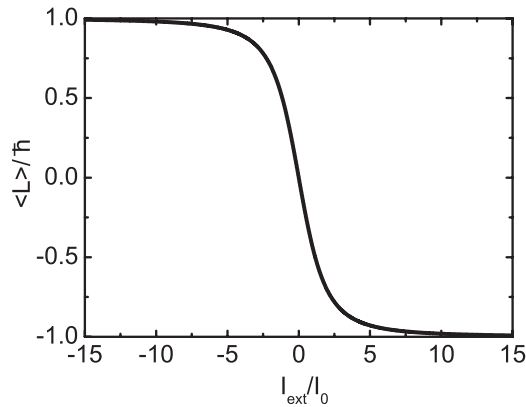


**Figure 2.** Expectation value  $\langle L \rangle$  of the cross-sectional angular momentum operator  $L$  of the twisted quantum ring. It decreases monotonically in response to an increase in the external current  $I_{\text{ext}}$  that penetrates within the ring (see figure 1).

limit of  $I_{\text{ext}} \rightarrow +\infty$  (or  $-\infty$ ). Furthermore, the decay in  $\langle L \rangle$  is steep only within the region  $-5 < I_{\text{ext}}/I_0 < 5$ . These features of  $\langle L \rangle$  imply that the torsion-induced phase shift  $\tau\langle L \rangle \ell / \hbar$  shows a significant response to the change in  $I_{\text{ext}}$  when  $I_{\text{ext}}$  lies within the region above. The flux-free interference effect in a helical circuit is a direct consequence of the torsion-induced phase shift, as demonstrated later.

### 3. Electron interferometer with a twisted quantum ring

Let us consider the conductance of a twisted-ring based interferometer measured by two terminals, as illustrated in figure 1. Two different paths connecting the two points P and Q have the same length of  $\pi R_1$ . The electron's path along two semi-infinite leads and the two semicircular arcs is parametrized by  $x$  such that  $x = 0$  at P and  $x = \pi R_1$  at Q; electron flow inserted from  $x = -\infty$  bifurcates at P, passing through either of the two branches (i.e., semicircles of the ring) until getting confluent at Q, and then flow away toward  $x = +\infty$ .

The wave functions  $\psi_s$  ( $s = 1, 2, 3, 4$ ) corresponding to the four different regions depicted in figure 1 are given by [44]

$$\begin{aligned}
 \psi_1(x) &= A_1 e^{ikx} + B_1 e^{-ikx}, \\
 \psi_2(x) &= A_2 e^{i(k+a)x} + B_2 e^{-i(k-a)x}, \\
 \psi_3(x) &= A_3 e^{i(k-a)x} + B_3 e^{-i(k+a)x}, \\
 \psi_4(x) &= A_4 e^{ikx}.
 \end{aligned} \tag{11}$$

Here,  $k$  is the wavenumber of the incident electron, and  $a \equiv \tau\langle L \rangle / \hbar$  is a wavenumber shift caused by  $I_{\text{ext}}$ .

The wavefunctions  $\psi_s$  satisfy the connection conditions:  $\psi_1 = \psi_2 = \psi_3$  and  $\partial_x \psi_1 = \partial_x \psi_2 + \partial_x \psi_3$  at P, and  $\psi_4 = \psi_2 = \psi_3$ ,  $\partial_x \psi_4 = \partial_x \psi_2 + \partial_x \psi_3$  at Q. Applying the conditions to equation (11), we obtain the conductance  $G$  of the system by using

the two-terminal Landauer formula [45],

$$G = \frac{2e^2}{h} |A_4|^2 = \frac{2e^2}{h} |(1 + \theta_1)A_2 + 2\theta_1(A_3 - 1)|^2, \quad (12)$$

where

$$A_2 = \frac{\alpha'\gamma - \beta\gamma'}{\alpha\alpha' - \beta\beta'}, \quad A_3 = -\frac{\beta'}{\alpha'}A_2 + \frac{\gamma'}{\alpha'}, \quad (13)$$

and

$$\begin{aligned} \alpha(k, a) &= k [2(2k + a) - (k + a)(\theta_2/\theta_1) + (k - a)\theta_2], \\ \beta(k, a) &= k [2k + a + (a/\theta_1) + 2(k - a)\theta_2], \\ \gamma(k, a) &= 2k[2k + a + (k - a)\theta_2], \end{aligned} \quad (14)$$

with the notations  $\theta_1 = \exp(-ik\ell)$ ,  $\theta_2 = \exp(ia\ell)$  and  $\xi'(k, a) = \xi(k, -a)$  for  $\xi = \alpha, \beta, \gamma$ . Once determining the dimensionless parameters  $k\ell$  and  $a\ell$  (or equivalently,  $k\ell$ ,  $\tau\ell$  and  $\langle L \rangle/\hbar$ ), we can evaluate  $G$  by using equations (12)-(14). If we impose  $a = 0$  in equation (14), the expression of  $G$  reduces to that of an ordinary un-twisted interferometer [44]

$$G = \frac{2e^2}{h} \frac{32}{41 - 9 \cos(k\ell)}. \quad (15)$$

To make concise arguments, we omit the electron's spin-dependent transport [46] nor impurities/structural disorder [47] in the system, though each of them is expected to yield interesting consequences similarly to the case of un-twisted systems.

## 4. Results

Figures 3 and 4 show the plots of the dimensionless conductance  $\tilde{G} \equiv G/(2e^2/h)$  as a function of the dimensionless current  $\tilde{I}_{\text{ext}} \equiv I_{\text{ext}}/I_0$  for various values of  $\tau\ell$  and  $k\ell$ . In figure 3 (or figure 4), we fix  $k\ell = 1.0$  (or  $\tau\ell = 1.0$ ) and choose several values of  $\tau\ell$  (or  $k\ell$ ) as indicated. In both figures, the curves of  $\tilde{G}$  exhibit waveforms within the region  $|\tilde{I}_{\text{ext}}| < 5$  but smooth (or almost constant) behaviors outside the region: The two contrasting features of  $\tilde{G}$  in the two regions are attributed to the nonlinear response in  $\langle L \rangle$  to  $I_{\text{ext}}$ , which will be discussed soon later.

The most important observation in figure 3 is an oscillation in  $\tilde{G}$  for large  $\tau\ell$ , which does not take place in figure 4. This conductance oscillation is what we call the flux-free interference effect, the peculiar phenomenon to the twisted-ring based AB interferometer. The magnitude of oscillation can be enhanced (i.e., the oscillation period is shortened) by increasing  $\tau\ell$ , since the larger  $\tau\ell$  results in the larger torsion-induced phase shift  $\tau\langle L \rangle\ell/\hbar$ . What value of  $\tau\ell$  should be required for observing the flux-free conductance oscillation strongly depends on the condition of  $k\ell$  we choose. When  $k\ell = 1.0$ , for instance, the oscillation disappears for  $\tau\ell \ll 10.0$  as shown in figure 3. An exhaustive study covering wide ranges of the parameter space makes clear the required values of  $\tau\ell$  and  $k\ell$ , which will be given elsewhere.

It is also noteworthy that the conductance oscillation in the present system is not periodic against the variation in  $I_{\text{ext}}$ , which differs from the ordinary AB effect driven by

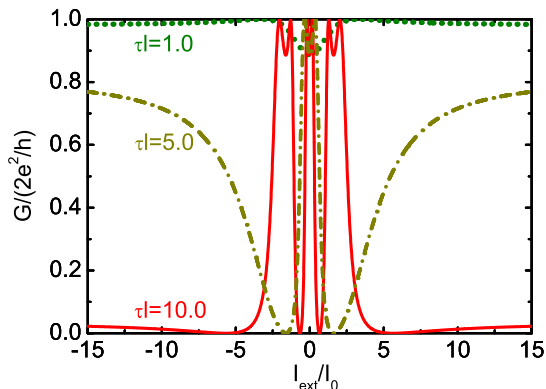


**Figure 3.** Dimensionless conductance  $G/(2e^2/h)$  as a function of the normalized external current  $I_{\text{ext}}/I_0$ . The parameter  $k\ell = 1.0$  is fixed for all curves that are each associated with different values of  $\tau\ell$ . An oscillation of  $G$  is observed around  $I_{\text{ext}} = 0$  at  $\tau\ell = 5.0, 10.0$ , and larger  $\tau\ell$  (not shown).

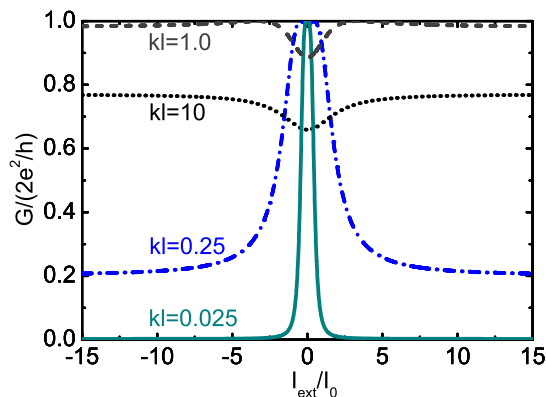


**Figure 4.**  $I_{\text{ext}}$ -dependence of  $G/(2e^2/h)$  with  $\tau\ell = 1.0$  being fixed. As  $k\ell$  increases, the width of the upward peak that initially arises at  $I_{\text{ext}} = 0$  becomes broader, and finally a slight hollow emerges at  $I_{\text{ext}} = 0$ .

penetrating magnetic flux. The non-periodic character is a consequence of the nonlinear dependence of  $\langle L \rangle$  on  $I_{\text{ext}}$  (see equation (10) and figure 2). We have seen from figure 2 that  $\langle L \rangle$  decreases steeply with increasing  $I_{\text{ext}}$  around  $I_{\text{ext}} \sim 0$  (at  $|I_{\text{ext}}| \gg 0$ ) and it decreases gently at the regions of  $|I_{\text{ext}}| \gg 0$ . This means that the phase shift  $\tau\langle L \rangle\ell/\hbar$  shows sensitive (insensitive) response to a change in  $I_{\text{ext}}$  at  $I_{\text{ext}} \sim 0$  ( $|I_{\text{ext}}| \gg 0$ ), and thus it reaches  $2\pi$  by only a small (very large) increase in  $I_{\text{ext}}$  at  $I_{\text{ext}} \sim 0$  ( $|I_{\text{ext}}| \gg 0$ ). As a result, the conductance oscillates densely (sparsely) at  $I_{\text{ext}} \sim 0$  ( $|I_{\text{ext}}| \gg 0$ ) since the oscillation stems from the quantum interference caused by the phase shift  $\tau\langle L \rangle\ell/\hbar$ .

As a by-product, we show in figure 4 the  $I_{\text{ext}}$ -dependence of  $G$  for a fixed  $\tau\ell$  ( $\tau\ell = 1.0$ ) and various  $k\ell$ . At  $k\ell \ll 1.0$ , a sharp peak arises at  $I_{\text{ext}} = 0$  whose peak width broadens gradually with increasing  $k\ell$ . The peak height at  $I_{\text{ext}} = 0$  is given

by equation (15), thus it oscillates with increasing  $k\ell$ . When  $k\ell$  exceeds 1.0, then  $G$  becomes almost constant over the range of  $I_{\text{ext}}$  we have considered, and it shows a slight hollow at  $I_{\text{ext}} = 0$ . The almost constant behavior of  $G(I_{\text{ext}})$  indicates that the torsion-induced phase shift gives little contribution to the motion of electrons whose energies are large enough to satisfy  $k\ell \geq 1.0$ .

## 5. Discussions

We remark that the numerical results in figures 3 and 4 are based on the presence of  $I_{\text{ext}}$  that threads the center of the ring. An experimental realization of such the setup may not be feasible in a straightforward manner, since the ring radius  $R_1$  should be small enough to keep the quantum coherence of mobile electrons. Still, we can build an equivalent setup to the above by applying an external magnetic field  $B_{\text{ext}}$ , instead of  $I_{\text{ext}}$ , to a portion of the ring in a *tangential* direction. This is because the tangential field  $B_{\text{ext}}$  engenders nonzero  $\langle L \rangle$  in the cross section and thus a phase shift in  $\psi(q_0)$ . A field strength of  $B_0 \sim 10\text{T}$  is required to observe the flux-free interference effect, provided the ring of the cross-sectional radius  $R_2 \sim 10\text{nm}$ ; we can estimate it from the relations of  $B_0 = \mu_0 I_0 / \ell = m^* \omega_p / e$  and  $\hbar \omega_p \sim m^* \omega_p^2 R_2^2 / 2$  (see Sec. 2). This field strength is accessible in the existing nanometric measurements, thus supporting an experimental feasibility of our results.

It is noticed that our attention has been limited to non-interacting electrons. When taking into account a Coulomb interaction between electrons, the amplitude of the conductance oscillation is expected to decrease to a degree. In fact, such the amplitude reduction caused by the Coulomb interaction was experimentally observed for un-twisted AB interferometers [48, 49], where sizeable interference patterns still remained to be obtained. A further interesting issue would be transport properties of the Tomonaga-Luttinger liquid (TLL) state in an AB interferometer. In one-dimensional systems, the slightest correlation between electrons can lead to the TLL states, a highly collective state of matter [50]. Recent studies have revealed that the conductance of TLL-based AB interferometers shows anomalous interference patterns that are substantially different from those of the ordinary (non-interacting) AB system [51, 52]. These facts pose a question as to what happens in the helical AB interferometer composed of the TLL states, which requires establishing newly the bosonization theory for a twisted quantum wire.

## 6. Conclusion

We theoretically predicted a non-trivial conductance oscillation in a twisted quantum ring that is free from threading magnetic flux. Helical atomic configuration inside the ring gives rise to a phase shift in the electron's eigenstates by  $\tau \langle L \rangle \ell / \hbar$ , where  $\tau$  the internal torsion of the ring,  $\langle L \rangle$  the angular momentum expectation value in the cross section, and  $\ell$  the ring perimeter. The phase shift induces the flux-free conductance



oscillation in response to a change in the external current  $I_{\text{ext}}$  or a tangential magnetic field  $B_{\text{ext}}$ , in which neither  $I_{\text{ext}}$  nor  $B_{\text{ext}}$  yields magnetic flux threading the ring. Our results suggest untouched quantum nature in actual low-dimensional nanostructures composed of helical atomic configuration.

## Acknowledgments

We would like to express our thanks to K Yakubo for illuminating discussions. One of the authors (HT) acknowledges K W Yu and M Arroyo for their comments and hospitalities during the stay in CUHK and UPC. HT also thanks the financial supports from the Japan Society for the Promotion of Science for Young Scientists and the Excellent Young Researcher Overseas Visit Program. This work is supported by a Grant-in-Aid for Scientific Research from the MEXT, Japan. Numerical calculations were performed in part by using the facility of Supercomputer Center, ISSP, University of Tokyo.

## References

- [1] Aharonov Y and Bohm D 1959 *Phys. Rev.* **115** 485
- [2] Tonomura A, Osakabe N, Matsuda T, Kawasaki T, Endo J, Yano S and Yamada H 1986 *Phys. Rev. Lett.* **56** 792
- [3] Caprez A, Barwick B and Batelaan H 2007 *Phys. Rev. Lett.* **99** 210401
- [4] Ionicioiu R 2003 *Phys. Rev. A* **68** 034305
- [5] Fischer A M, Campo V L Jr., Portnoi M E and Römer R A 2009 *Phys. Rev. Lett.* **102** 096405
- [6] Schwingenschlögl U and Schuster C 2008 *J. Phys.: Condens. Matter* **20** 383201
- [7] Cano A and Paul I 2009 *Phys. Rev. B* **80** 153401
- [8] Aharonov Y and Casher A 1984 *Phys. Rev. Lett.* **53** 319
- [9] Cimmino A, Opat G I, Klein A G, Kaiser H, Werner S A, Arif M and Clothier R 1989 *Phys. Rev. Lett.* **63** 380
- [10] Sangster K, Hinds E A, Barnett S M and Riis E 1993 *Phys. Rev. Lett.* **71** 3641
- [11] He X-G and McKellar B H J 1993 *Phys. Rev. A* **47** 3424
- [12] Wilkens M 1994 *Phys. Rev. Lett.* **72** 5
- [13] Dowling J P, Williams C P and Franson J D 1999 *Phys. Rev. Lett.* **83** 2486
- [14] Cook R J, Fearn H and Milonni P W 1995 *Am. J. Phys.* **63** 705
- [15] Haldane F D M and Wu Y-S 1985 *Phys. Rev. Lett.* **55** 2887
- [16] Kivelson S A and Spivak B Z 1992 *Phys. Rev. B* **45** 10490
- [17] Sonin E B 1997 *Phys. Rev. B* **55** 485
- [18] Mel'nikov A S 2001 *Phys. Rev. Lett.* **86** 4108
- [19] Ford L H and Vilenkin A 1981 *J. Phys. A* **14** 2353
- [20] Reznik B 1995 *Phys. Rev. D* **51** 3108
- [21] Bakke K and Furtado C 2009 *Phys. Rev. D* **80** 024033
- [22] Cotaescu I I and Papp E 2007 *J. Phys.: Condens. Matter* **19** 242206
- [23] Barwick B and Batelaan H 2008 *New J. Phys.* **10** 083036
- [24] Takagi S and Tanzawa T 1992 *Prog. Theor. Phys.* **87** 561
- [25] Mitchell K A 2001 *Phys. Rev. A* **63** 042112
- [26] Éntin M V and Magarill L I 2002 *Phys. Rev. B* **66** 205308
- [27] Longhi S 2009 *Laser and Photon. Rev.* **3** 243
- [28] Cohen-Karni T, Segev L, Srur-Lavi O, Cohen S R and Joselevich E 2006 *Nature Nanotech.* **1** 36

- [29] Nagapriya K S, Goldbart O, Kaplan-Ashiri I, Seifert G, Tenne R and Joselevich E 2008 *Phys. Rev. Lett.* **101** 195501
- [30] Balakrishnan R and Dandoloff R 2007 *Nonlinearity* **21** 1
- [31] da Fonseca A F and Galvão D S 2008 *Phys. Rev. Lett.* **92** 175502
- [32] Arias I and Arroyo M 2008 *Phys. Rev. Lett.* **100** 085503
- [33] Wang Z, Zu X, Gao F and Weber W J 2008 *Phys. Rev. B* **77** 224113
- [34] Vassilev V M, Djondjorov P A and Mladenov I M 2008 *J. Phys. A.: Math. Theor.* **41** 435201
- [35] Jensen H and Koppe H 1971 *Ann. Phys.* **63** 586
- [36] da Costa R C T 1981 *Phys. Rev. A* **23** 1982
- [37] Taira H and Shima H 2010 *J. Phys.: Condens. Matter* **22** 075301
- [38] Taira H and Shima H 2007 *Surf. Sci.* **601** 5270
- [39] Shima H, Yoshioka H and Onoe J 2009 *Phys. Rev. B* **79** 201401(R)
- [40] Ono S and Shima H 2009 *Phys. Rev. B* **79** 235407
- [41] Atanasov V, Dandoloff R and Saxena A 2009 *Phys. Rev. B* **79** 033404
- [42] Fock V 1928 *Z. Phys.* **47** 446
- [43] Darwin C G 1930 *Proc. Camb. Philos. Soc.* **27** 86
- [44] Yakubo K and Ohe J 2000 *J. Phys. Soc. Jpn.* **69** 2170
- [45] Hod O, Baer R and Rabani E 2008 *J. Phys.: Condens. Matter* **20** 383201
- [46] Ying Y, Jin G and Ma Y 2009 *J. Phys.: Condens. Matter* **21** 275801
- [47] Heinrichs J 2009 *J. Phys.: Condens. Matter* **21** 295701
- [48] Tarucha S, Honda T and Saku T 1995 *Sol. Stat. Comm.* **94** 413
- [49] Ihnatsenka S and Zozoulenko I V 2008 *Phys. Rev. B* **77** 235304
- [50] Voit J 1995 *Rep. Prog. Phys.* **58** 977
- [51] Aristov D N and Wölfle P 2009 *Phys. Rev. B* **80** 045109
- [52] Krive I V, Palevski A, Shekhter R I and Jonson M 2010 *Low Temp. Phys.* **36** 119